

Investigation of the electron-electron scattering in tungsten

I. F. Voloshin, V. A. Gasparov, S. V. Kravchenko, and L. M. Fisher

Institute of Solid-State Physics, Academy of Sciences of the USSR, Chernogolovka, Moscow Province

V. I. Lenin All-Union Electrical Engineering Institute, Moscow

(Submitted 8 August 1986)

Zh. Eksp. Teor. Fiz. **92**, 745–755 (February 1987)

The temperature dependence of the collision frequency $\bar{\nu}(T)$ of electrons on central and noncentral sections of the Fermi surface of tungsten was investigated using the rf size effect in magnetic fields parallel and perpendicular to the surface of a sample. The dependence $\bar{\nu}(T) = \alpha T^2 + \beta T^3$ with an isotropic coefficient α and an anisotropic coefficient β described well the independent contributions of the electron-electron and electron-phonon scattering, respectively. The value of α was independent of thickness and purity of the samples and was the same for a hole octahedron and an electron "jack." For an electron spheroid the coefficient α was 1.5 times higher. Moreover, α was independent of a strong magnetic field, indicating the absence of a contribution of the electron-paramagnon scattering to α . The results obtained are in good agreement with the transport collision frequency and with theoretical calculations of the electron-electron scattering on various sheets of the Fermi surface of tungsten.

1. INTRODUCTION

The rf size effect (RSE) is due to a narrow belt of electrons on the Fermi surface. Therefore, the electron collision frequency $\bar{\nu}(T)$ measured by the RSE method is equally sensitive to normal electron-electron (*ee*) collisions and to umklapp scattering.¹ Consequently, a study of the *ee* scattering in metals by the RSE method has important advantages compared with the dc measurements.²

Investigations of the temperature dependence of the collision frequency $\bar{\nu}(T)$ of electrons in Mo carried out using the RES method in magnetic fields \mathbf{B} parallel³ and perpendicular⁴ to the surface of a sample have shown that $\bar{\nu}(T) = \alpha T^2$, where the coefficient α is independent of the purity and thickness of the samples and is not greatly affected by the positions of the orbits on different sheets of the Fermi surface. It has been concluded on the basis of these results that the quadratic term in $\bar{\nu}(T)$ is due to the *ee* scattering in this metal. Observation of hot electrons in Mo also agrees with the high frequency of the *ee* collisions in this metal.⁵

As in other compensated metals, the temperature dependence of the electrical resistivity $\rho(T)$ of Mo should include a contribution not only from the umklapp *ee* scattering, but also from normal electron-hole collisions.^{1,2} However, since the scattering angles for the *ee* collisions are large, there should be a correlation between the quadratic contributions to the transport and total collision frequencies. In fact, it has been found that α agrees well with the coefficient a which occurs in front of the quadratic term in the temperature dependence of the electrical resistivity of Mo described by $\rho(T) = aT^2 + bT^5$ and due to the *ee* scattering.³ The quadratic temperature dependence of the collision frequency $\bar{\nu}(T)$ of electrons in Mo follows also from the experiments on the attenuation of ultrasound.⁶

It is natural to expect manifestation of the *ee* collisions also in the case of W, which belongs to the same chromium group and is an electronic analog of Mo. However, the RSE investigations^{1,7} have shown that the dependence $\bar{\nu}(T)$ exhibited by W is more complex than that of Mo. At helium temperatures it is described by the law αT^2 and at higher

temperatures it obeys βT^3 . The complexity of the dependence $\bar{\nu}(T)$ had led to incorrect conclusions on the anisotropy of the *ee* collision probability for a hole octahedron of the Fermi surface of W (Ref. 7). Moreover, a study of $\rho(T)$ has revealed surface-induced deviations from the Matthiessen rule. It has thus been found that the coefficient a is strongly sensitive to the purity, thickness d , and the state of the surface of single crystals of W (Refs. 8 and 9). Extrapolation of a to the limit $d \rightarrow \infty$ in accordance with the law $(l/d)^{2/3}$ yielded $a \rightarrow 0$ (l is the mean free path of carriers). However, experiments carried out at $T < 1$ K (Ref. 10), which showed that $\rho(T) = aT^2$, and several other investigations established that $a \rightarrow 5 \times 10^{-13} \Omega \cdot \text{cm} \cdot \text{K}^{-2}$ in the limit $d \rightarrow \infty$ (Ref. 11). Moreover, the law $(l/d)^{2/3}$ is valid only in the range $l > d$ so that extrapolation of a in accordance with this law to the limit $d \rightarrow \infty$ is unjustified.¹¹ According to Refs. 8 and 9, the dependence $a(l/d)$ is very weak in the case of Mo.

The physical nature of the quadratic term in the dependence $\bar{\nu}(T)$ obtained for W was identified by detailed investigations of $\bar{\nu}(T)$ which we carried out on this metal using the RSE method in magnetic fields parallel (weak \mathbf{B}) and perpendicular (strong \mathbf{B}) to the surface of a sample. Application of the RSE in a perpendicular magnetic field (Gantmakher-Kaner effect) was of interest not only from the point of view of investigation of the dependence $\bar{\nu}(T)$ by a different method and determination of α for a noncentral section of the hole octahedron of the Fermi surface, but also in relation to the dependence $\alpha(B)$. This was due to the fact that the quadratic term in the dependence $\bar{\nu}(T)$ could also, in principle, be due to the scattering of electrons by spin fluctuations (paramagnons).¹² A strong magnetic field should suppress paramagnons and the scattering mechanism could then be determined.

2. EXPERIMENTS

1. Experiments in a field \mathbf{B} parallel to the surface of a sample were carried out using a modulation method for recording the RSE lines. We determined the first derivative of the active part of the surface impedance $\partial R / \partial B$ on B . The apparatus and the investigation method were described in

detail earlier.^{1,3} In determination of the dependence $\bar{\nu}(T)$ the precision of measurements of the amplitude A of the RSE line was improved considerably compared with the earlier investigations.^{1,13} This was done by connecting a G-1212:010 digital millivoltmeter parallel to the y input of an Endim 620.02 XY plotter. Slow variation of the magnetic field with a Varian electromagnet allowed us to determine the RSE line amplitudes in digital form with an error an order of magnitude less than in the determination from the records obtained with the plotter. Averaging of three to five sets of results at each temperature also increased the precision, particularly when weak RSE lines were recorded.

Considerable attention was given to the precision of the stabilization of the temperature T at $T < 4.2$ K. With this in mind a vacuum jacket of a sample holder³ was filled with liquid helium and temperature was stabilized not only with the aid of the pumping rate, but also using a heater. Temperature was measured employing an Allen-Bradley carbon resistor calibrated using a CR 1000-1.5-100 secondary standard. Consequently, the error in the temperature determination did not exceed $\pm 0.2\%$ and the dependence $A(T)$ was found to within $\pm 1-2\%$. The experiments were carried out in the frequency interval 1.5–8 MHz at temperatures $1.25 < T \leq 10$ K.

2. The collision frequency $\bar{\nu}(T)$ was deduced from the RSE data in a perpendicular field in the same way as in Ref. 4. Measurements at temperatures $T > 4.2$ K were carried out employing an "anticryostat" where a sample with a heater was placed. This anticryostat was filled with gaseous helium at atmospheric pressure. Thermal contact between the sample and the helium bath was provided by a helium heat exchanger located in the space between the walls of the anticryostat. The temperature of the sample was kept constant by an automatic temperature regulator. An Allen-Bradley resistance thermometer was used as the sensor. Temperatures below 4.2 K were stabilized by controlling the ⁴He vapor pumping rate. The temperature interval was increased compared with Ref. 13 to 1.5–9 K.

In these experiments we determined the amplitude A of the oscillations of the second derivative of the active part of the surface impedance $\partial^2 R / \partial B^2$ recorded in the $\mathbf{B} \parallel \mathbf{n} \parallel \langle 100 \rangle$ configuration (\mathbf{n} is the normal to the surface of a sample). The rf field was circularly polarized (negative polarization). In this case the oscillations were due to the RSE of resonance holes located on a noncentral section of the octahedron.¹⁴ At the same time the real $R(B, T)$ and imaginary $X(B, T)$ parts of the surface impedance $Z = R - iX$ were recorded. Measurements were carried out in strong fields because, according to the theory of Ref. 14, the frequency $\bar{\nu}(T)$ was independent of B for different serial numbers of the oscillations. This was confirmed by a special investigation. The frequency interval was 100–500 kHz. The error in the determination of $\bar{\nu}(T)$ did not exceed 5–10%.

3. The investigated samples were cut by spark machining from a single-crystal tungsten ingot. The electrical resistivity ratio was determined from the decay of eddy currents in a rotating magnetic field. For samples d_1-d_3 this ratio was $\rho_{300\text{K}} / \rho_{4.2\text{K}} \approx 7.5 \cdot 10^4$ ($\rho_{300\text{K}} / \rho_{0\text{K}} \approx 1 \cdot 10^5$),¹¹ whereas for sample d_4 we found that $\rho_{300\text{K}} / \rho_{4.2\text{K}} = 3.5 \cdot 10^4$. Disks oriented in the (100) plane by the Laue x-ray diffraction method had a diameter of 6–7 mm and were treated by a method described in Ref. 15. The direction of the normal \mathbf{n} of such

samples coincided with the $\langle 100 \rangle$ axis to within $\pm 1^\circ$. The high purity of W made it possible to observe the RSE oscillations in fairly thick samples: $d_1 = 1.3$ mm, $d_2 = 1.87$ mm, $d_3 = 2.82$ mm, and $d_4 = 2$ mm.

Special care was taken in the RSE measurements to ensure that the field \mathbf{B} was parallel exactly to the surface of a sample. A special device and the dependence of A on the tilt of the field were used to set \mathbf{B} parallel to the surface to within $\pm 10'$. Lowering of the helium level resulted in a slight tilt of a sample for mechanical reasons, so that the parallel orientation of \mathbf{B} was monitored continuously during an experiment. This aspect was ignored in the previous investigations, giving rise to inaccuracies in the experimental data on the RSE lines characterized by a strong dependence of A on the tilt of \mathbf{B} (Refs. 13 and 16).

Investigations of the dependence of the RSE oscillation amplitude in a perpendicular field on d showed that $l \approx 1$ mm at $T = 4.2$ K for samples d_1-d_3 (Ref. 15) and $l \approx 0.7$ mm for sample d_4 . For this reason the amplitudes of the RSE lines and oscillations obtained for sample d_3 were low. Moreover, the thickness of sample d_3 was only half the diameter, which resulted in an inhomogeneity of the distribution of the rf field on the surface of the sample and possible errors in the impedance measurements. When the field was parallel, the RSE lines of sample d_3 were observed in weak magnetic fields against the background of a strong nonmonotonic dependence $\partial R(B) / \partial B$ which was due to the zeroth line. These problems were not encountered for thinner samples and the extremely small line width $\Delta B / B \approx 1\%$ allowed us to ignore the changes in the envelope with temperature. Consequently, the experiments were carried out mainly on samples $d_1, d_2,$ and d_4 .

3. RESULTS OF MEASUREMENTS

Figure 1 shows examples of RSE lines recorded in a parallel field. Detailed investigations of the Fermi surface of W by the RSE method reported in Ref. 15 allowed us to attribute these lines to various orbits on the Fermi surface. It

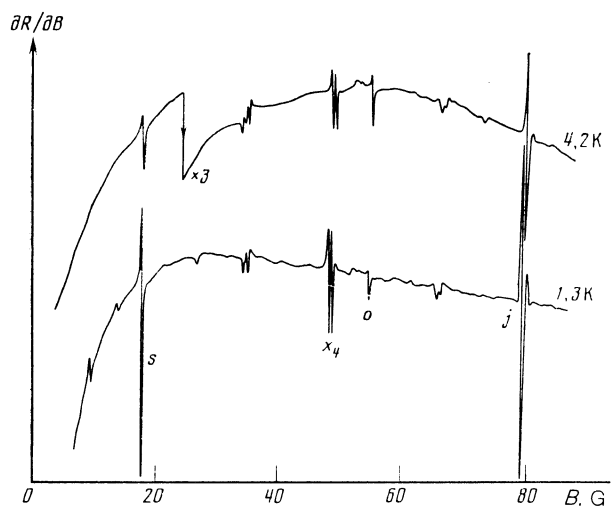


FIG. 1. Examples of the RSE lines recorded in a parallel magnetic field for sample d_2 ; $\omega/2\pi = 2.5$ MHz. The symbols s , o , and j represent the lines due to the cyclotron orbits on the spheroid, octahedron, and jack of the Fermi surface, respectively. Comments on the line x_4 can be found in the text. In the course of recording these curves at 4.2 K the amplification was increased threefold after the spheroid line.

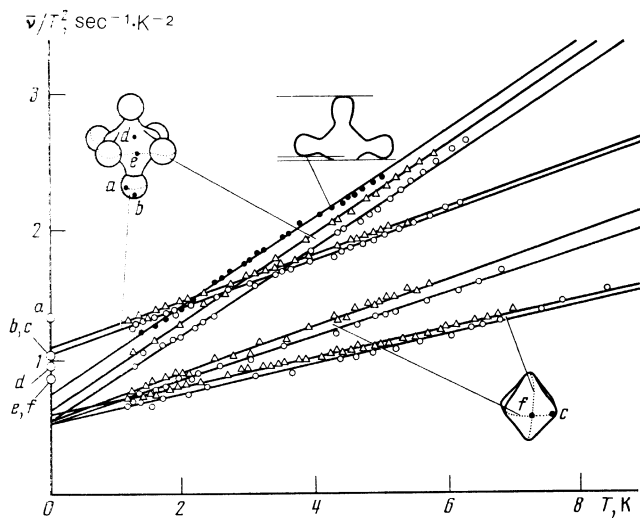


FIG. 2. Dependence of $\bar{\nu}/T^2$ on T for different RSE lines in a parallel magnetic field. The dotted curves in the inset show the investigated orbits. The pointers identify the pairs of neighboring straight lines and the orbits for which the results were obtained. The symbols \circ and Δ represent the dependences obtained for samples d_1 and d_2 , respectively; the symbol \bullet gives the results of the x_4 line of sample d_2 . The points, a, b, c, d, e, and f are the states on the Fermi surface for which the ee collision frequencies, identified on the ordinate axis, are calculated in Ref. 28.

is clear from Fig. 1 that the line width was considerably less than in Ref. 15, which increased considerably the precision in the determination of the radius vectors of the Fermi surface. Special investigations of the anisotropy of the positions of the RSE lines confirmed completely all the earlier¹⁵ conclusions on the topology and dimensions of the Fermi surface of W. These results were in good agreement with the theoretical calculations of the Fermi surface reported in Refs. 17 and 18.

In the RSE experiments in a parallel field the line amplitude could include contributions from repeated return of electrons to the skin layer (multirevolution effect) in the case when $l > d$. Under these conditions the relationship between A and $\bar{\nu}(T)$ was very complex and it had been discussed frequently in several reviews.^{19,20} Numerical calculations and experimental investigations showed that even when $l = 2d$ the contribution of the multirevolution effect to A did not exceed 10% (Ref. 20). Moreover, experiments carried out on Mo showed that if $d > l$, then the function $\bar{\nu}(T)$ obtained from a formula ignoring the multirevolution effect was the same for samples of different thickness.³

Since the present investigation was carried out under conditions corresponding to $d > l$, the temperature dependence of the electron collision frequency averaged over the

Fermi surface section with an extremal diameter was analyzed using the formula

$$\bar{\nu}(T) = \oint \frac{v(\mathbf{k}) d\mathbf{k}}{v_{\perp}(\mathbf{k})} / \oint \frac{d\mathbf{k}}{v_{\perp}(\mathbf{k})} = \frac{1}{t} \frac{\ln A(0)}{\ln A(T)}, \quad (1)$$

valid in the case of single traversal of an electron of a path from one side of the sample to the other, i.e., valid in the case when $\bar{\nu}_0 + \bar{\nu}(T) > \Omega$, where $\bar{\nu}_0$ is the frequency of collisions with static defects of the crystal lattice. Here, $v_{\perp}(\mathbf{k})$ is the projection of the Fermi velocity on the plane of an orbit at the point \mathbf{k} of the Fermi surface, $t = \pi/\Omega$ is half the cyclotron period of the electrons revolving at a frequency $\Omega = eB/m^*c$, e is the electron charge, c is the velocity of light, m^* is the cyclotron mass, and $A(0)$ is the RSE line amplitude at $T = 0$. This formula (1) is valid if the widths and profiles of the RSE lines remain constant when temperature is varied, which was checked in the course of our measurements.

The dependence $A(T)$ was investigated in the case of four different RSE lines due to extremal orbits of the hole octahedron (O), electron spheroid (s), and "jack" (j) of the Fermi surface of W for the $\mathbf{B} \parallel \langle 100 \rangle$ and $\mathbf{B} \parallel \langle 110 \rangle$ configurations when the orbits passed through all the main sections of the Fermi surface (see Figs. 1 and 2 and Table I). Moreover, an independent check of the validity of Eq. (1) was made by investigating the dependence $\bar{\nu}(T)$ for the x_4 line (Ref. 15) due to an open cyclotron orbit. It is clear from Fig. 1 that the x_4 line was split. An analysis indicated that such splitting was due to a tilt of \mathbf{n} from the $\langle 100 \rangle$ axis by an angle $\approx 1^\circ$. It is clear from the shape of the corresponding orbit shown as an inset in Fig. 2 that for this tilt there were two extremal sizes of the orbits and an electron could pass only once from one side of the sample to the other. Unfortunately, the amplitudes of the RSE lines due to the ellipsoids were very low (Fig. 1) and were observed in very weak magnetic fields against the background of the nonmonotonic dependence $\partial R(B)/\partial B$, which limited the precision of our measurements. Therefore, these lines were not used in our investigation of $\bar{\nu}(T)$.

In the (110) plane the orbits of the effective electrons on the octahedron and jack had an extended flat region in the skin layer and, consequently, the time of flight t from one side of the sample to the other was less than π/Ω (Ref. 3). Therefore, the experiments were carried out only in the (100) plane, in spite of the much lower amplitudes of the RSE lines. It should be noted that in the preceding investigations this circumstance was ignored, which led to incorrect conclusions on the anisotropy of the quadratic term in the dependence $\bar{\nu}(T)$ (Refs. 1 and 7).

TABLE I.

Surface	Directions of \mathbf{B}	$ \mathbf{k}_z $, \AA^{-1}	m^*/m_0	α , $10^7 \text{ sec}^{-1} \cdot \text{K}^{-2}$	β , $10^7 \text{ sec}^{-1} \cdot \text{K}^{-3}$
Octahedron	$\langle 100 \rangle$	$\begin{cases} 0 \\ 0.22 \end{cases}$	$\begin{cases} 1.03 \\ 0.70^* \end{cases}$	$\begin{cases} 0.55 \\ 0.65 \end{cases}$	$\begin{cases} 0.16 \\ 0.19 \end{cases}$
	$\langle 110 \rangle$	0	0.68	0.54	0.11
Jack	$\langle 100 \rangle$	0	2.2	0.62	0.34
Spheroid	$\langle 100 \rangle$	0	0.57	1.1	0.18

Note. *Our values; m_0 is the mass of a free electrons and \mathbf{k}_z is the projection of the wave vector of an electron along the $\mathbf{B} \parallel z$ direction.

Table I gives the cyclotron masses m of the carriers deduced from the de Haas–van Alphen effect²¹ and from the cyclotron resonance^{22,23} and used in the calculations of $\bar{v}(T)$ on the basis of Eq. (1), together with the results of measurements of the coefficients α and β .

In the RSE experiments we determined the total probability of electron collisions. Assuming that the contributions to the ee and electron-phonon (ep) collisions were independent and additive, we concluded that $\bar{v}(T) = \alpha T^2 + \beta T^3$. On this assumption we analyzed the experimental data using the following formula:

$$\ln A(T) = \ln A(0) - \alpha t T^2 - \beta t T^3. \quad (2)$$

A computer analysis of the dependence $A(T)$ by the least-squares method made it possible to determine the constant $A(0)$ as well as the coefficients α and β . Figure 2 shows the dependences of $\bar{v}(T)/T^2$ on T for all the investigated orbits in samples d_1 and d_2 . In this graph the constant cutoff on the ordinate gives α and the slope of the straight lines gives β . Table I gives the average results for two samples.

For comparison, Fig. 2 shows the dependence of $\bar{v}(T)/T^2$ on T for the x_4 line due to an open cyclotron orbit on the jack in the case when $\mathbf{B} \parallel \langle 100 \rangle$ (see the inset), which—as pointed out above—is not affected by the multirevolution effect. We can easily demonstrate that if $v_{\perp} = \text{const}$, then the transit time for such an orbit is $t = eBL_1/\pi m^* c L_0$, where L_1 is the perimeter of half the investigated orbit and L_0 is the perimeter of half the cyclotron orbit j in the field \mathbf{B} . According to Ref. 15, we have $L_1/L_0 = 0.59$. We are assuming that m^* is $m^* = 2.2m_0$ for a closed orbit. We can see that the dependence $\bar{v}(T)$ for x_4 is the same as for a closed orbit and a slight quantitative difference of α is clearly due to indeterminacy of t .

Oscillations of the RSE in a perpendicular magnetic field $\mathbf{B} \parallel \langle 100 \rangle$ applied to W are due to a noncentral section of the hole octahedron corresponding to the value of k_z for which the derivative $\partial S/\partial k_z$ has an extremum. Here, $S(k_z)$ is the area of a section of the Fermi surface by a plane perpendicular to \mathbf{B} .

The width of the belt Δk_z of resonance carriers depends on the sharpness of the extremum of $\partial S/\partial k_z$, on the thickness of the sample, and on the applied magnetic field:

$$\Delta k_z = 2 \left\{ \left(\frac{\partial S}{\partial k_z} \right)_{\text{ext}} \left/ \frac{\partial^2 S}{\partial k_z^2} k_{\text{GK}} d \right. \right\}^{1/2}, \quad (3)$$

where

$$k_{\text{GK}} = 2\pi/u_{\text{ext}}, \quad u_{\text{ext}} = \hbar c (\partial S/\partial k_z)_{\text{ext}}/eB,$$

and K_{GK} is the wave vector of the Gantmakher-Kaner component. Under the experimental conditions the width Δk of the belt is of the order of 10^{-2} \AA^{-1} . The collision frequency $\bar{v}(T)$ averaged over the orbit belt for this section was found from the formula⁴

$$\bar{v}(T) = \frac{v_z}{d} \left[\ln \frac{A(0)}{|Z(0)|^2} - \ln \frac{A(T)}{|Z(T)|^2} \right] = \alpha T^2 + \beta T^3, \quad (4)$$

where $|Z(B, T)|^2 = R^2(B, T) + X^2(B, T)$ is the square of the modulus of the surface impedance of the sample, $A(B, T)$ is the oscillation amplitude, and $v_z = \hbar(\partial S/\partial k_z)/2\pi m^*$ is the longitudinal component of the average electron velocity on an extremal section. We can find m^* for this section from the dependence of $dS/\partial k_z$ on k_z calculated for $\mathbf{B} \parallel \mathbf{z}$ on a comput-

er employing a program given in Ref. 24. We introduced an analytic description of the radius vector $k(\theta, \varphi)$ for the hole octahedra of W in the form of a series of nine cubic harmonics:

$$k^2(\theta, \varphi) = \sum_l d_l K_l(\theta, \varphi),$$

where l is the order of the harmonic $K_l(\theta, \varphi)$ and d_l are the coefficients in the expansion obtained from the inversion of the data on the de Haas–van Alphen effect.²¹ Calculations showed that the function $|\partial S(k_z)/\partial k_z|$ passes through its maximum value of 3.73 \AA^{-1} at $k_z = 0.13 \text{ \AA}^{-1}$. The same result was obtained earlier using a similar representation $k(\theta, \varphi)$ in the form of a series of twelve cubic harmonics when other experimental data were inverted.²⁵ The experimental values deduced from the RSE $|\partial S/\partial k_z| = 3.13 \text{ \AA}^{-1}$ (Ref. 14) and from the Sondheimer effect, 2.95 \AA^{-1} (Ref. 25), were found to be 25% less than the calculated value, indicating that the analytic description of the hole octahedron by a series of cubic harmonics was clearly insufficient for the calculation of the derivatives $\partial S(k_z)/\partial k_z$.

In fact, the calculations reported in Ref. 25 in accordance with a three-parameter model of the octahedron gave the value $|\partial S/\partial k_z| = 3.04 \text{ \AA}^{-1}$, in good agreement with the experimental results. It is important to note that this extremum of $\partial S/\partial k_z$ corresponds to $k_z = 0.22 \text{ \AA}^{-1}$. This gives a more accurate position of the k_z section. The value of $m^* = (\hbar/2\pi) \oint v_{\perp}^{-1}(\mathbf{k}) d\mathbf{k}$ for this section was determined by numerical integration on a computer. Use was made of an analytic representation of the Fermi velocities on the hole octahedron also in the form of a series in cubic harmonics:

$$v_x(\theta, \varphi) = 2 \left[\sum_l d_l K_l(\theta, \varphi) \right]^{1/2} / \sum_l b_l K_l(\theta, \varphi). \quad (5)$$

This representation is obtained in the case of inversion of the data on the anisotropy of the cyclotron masses on the central sections of the octahedron.²¹ The value of m^* on this section with an extremal $\partial S/\partial k_z$ is $0.70m_0$, and the velocity is $v_z = 0.818 \times 10^8 \text{ cm/sec}$.

Examples of records of the oscillations of the surface resistance $\partial^2 R/\partial B^2$ obtained in a narrow range of magnetic fields are plotted in Fig. 3. These oscillations were a harmonic function of the field. Their amplitude increased approximately 50-fold as temperature was lowered from 9.1 K to 1.5 K. Even at the highest temperature of 9.1 K the noise did not exceed 10% of the peak-to-peak amplitude of the oscillations.

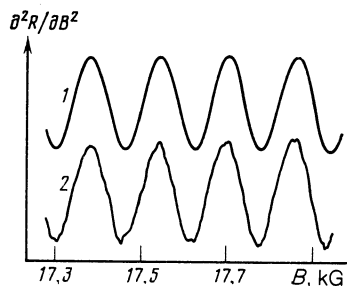


FIG. 3. Fragments of oscillations of $\partial^2 R/\partial B^2$ at temperatures 1.55 K (curve 1) and 9.1 K (curve 2); $d = 1.3 \text{ mm}$, $\omega/2\pi = 500 \text{ kHz}$. The gain used to record curve 2 was 50 times higher than that for curve 1.

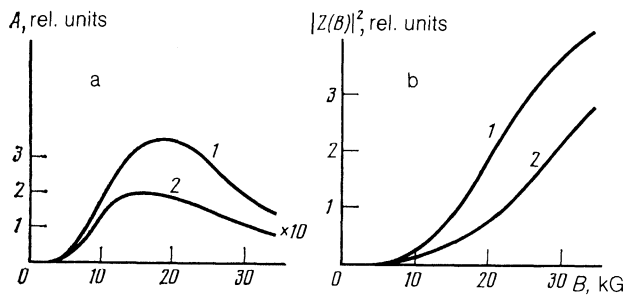


FIG. 4. Oscillation amplitude A (a) and square of the modulus of the impedance $|Z|^2$ (b) plotted as a function of the magnetic field; $d = 1.3$ mm, $\omega/2\pi = 500$ kHz. Curves denoted by 1 correspond to $T = 4.23$ K and curves denoted by 2 correspond to 8.5 K.

tions. Since in a sufficiently strong field ($B \gtrsim 15$ kG at $f = 500$ kHz) the collision frequencies were practically the same when calculated from different oscillation extrema, the precision of the results was improved by averaging the dependences $\bar{\nu}(T)$ for several neighboring extrema. The dependences of $|Z|^2$ and A on the magnetic field occurring in Eq. (4) are plotted for two temperatures in Fig. 4.

The experimental data on $\bar{\nu}(T)/T^2$ plotted as a function of T are shown in Fig. 5; they represent the results of an analysis obtained by the application of Eq. (4) to the data on samples d_1 , d_2 , and d_4 . The results for sample d_4 were obtained in a narrower temperature range ($1.5 \leq T \leq 5$ K). In the case of this sample the mean free path l was insufficiently large and at temperatures $T > 5$ K the signal/noise ratio decreased so much that the precision of the determination of $\bar{\nu}(T)$ was unsatisfactory. Clearly, within the limits of the experimental error, the dependence $\bar{\nu}(T)$ was the same for all the samples. The values of α and β averaged on the basis of these data are listed in Table I. Some discrepancy between these data and those given in Ref. 13 is due to, firstly, a different value of m^* and, secondly, the wider temperature range and the correspondingly higher precision in the determination of $\ln[A(0)/|Z(0)|^2]$ in the present study.

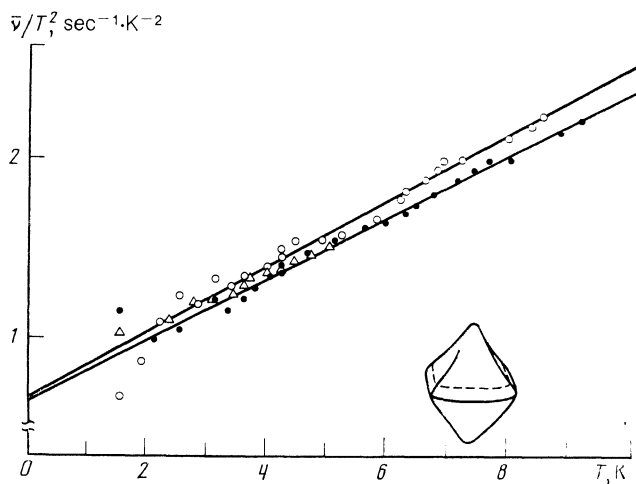


FIG. 5. Dependences $\bar{\nu}/T^2$ on T for a noncentral section of the hole octahedron (see inset). The symbols \bullet , \circ , and Δ represent the dependences for samples d_1 , d_2 , and d_4 , respectively.

4. DISCUSSION OF RESULTS

It is clear from the data presented in Figs. 2 and 5 that the dependences $\bar{\nu}(T)$ are described well by a sum of two terms: $\bar{\nu}(T) = \alpha T^2 + \beta T^3$. The coefficient α is practically independent of d and of the positions of the orbits on the main sheets of the Fermi surface of W. It should be noted that the transit times t then differ severalfold. The cubic term is strongly anisotropic, which is associated with the anisotropy of the ep collisions, well known in the case of noble metals (see, for example, Ref. 26). The lack of proportionality between the ratio α/B for the open and closed orbits on the electron jack is probably also associated with this anisotropy.

The coefficient α for the electron orbits on a noncentral section of the hole octahedron is in good agreement with the data for central sections and is independent of l . This circumstance is very important because it implies independence of α on B , and demonstrates the absence of the contributions of the electron-paramagnon scattering sensitive to a strong magnetic field.¹²

As pointed out above, earlier RSE investigations of the dependence $\bar{\nu}(T)$ for W were carried out in a parallel field¹⁻⁷ applied in the (110) plane, for which the time of flight is $t < \pi/\Omega$. Therefore, it is difficult to compare these previous investigations with our results (see Ref. 3). However, such effects are unimportant in the case of the spheroid, for which it is found in Ref. 1 that $\alpha = 1.3 \times 10^7 \text{ sec}^{-1} \cdot \text{K}^{-2}$. Bearing in mind the precision of the measurements reported in Ref. 1, we find that this value is in good agreement with our results. Since the resistivity ratio of the samples used in Ref. 1 was $\rho_{300\text{K}}/\rho_{4.2\text{K}} = 3.5 \cdot 10^4$, this comparison shows also that α is independent of the purity of the samples.

In the Born approximation the frequency of the normal ee collisions determined by the RSE method and corrected for the scattering by the screened Coulomb potential is given by the expression³

$$\bar{\nu}_{ee}(T) = \frac{4}{3} \pi \left(\frac{e}{\hbar} \right)^4 \frac{k^2}{v^3 g^2} \left(\frac{2k}{4k^2 + g^2} + \frac{1}{g} \arctg \frac{2k}{g} \right) (k_B T)^2, \quad (3)$$

where k_B is the Boltzmann constant, $g^{-1} = [4\pi e^2 N(\epsilon_F)]^{-1/2}$ is the screening radius, and $N(\epsilon_F)$ is the density of the electron states at the Fermi level. It follows from Eq. (6) that $\bar{\nu}_{ee} \propto k/v^3$. Table II gives the Fermi velocities and the corresponding values of k for the Fermi surfaces of W and Mo (Refs. 15, 21, and 27).

The values of $\bar{\nu}$ and \bar{k} are averaged over the cyclotron orbit for the central section of the corresponding sheet of the Fermi surface for the selected direction of \mathbf{B} . We can easily see that in the case of the spheroid the ratio k/v^3 is 2.8 times greater than for the hole octahedron. However, in fact we need allow not only for the intraband ee collisions, but also for the interband scattering with transfer to the neighboring semisurface sheets, as was done for the case of Mo in Ref. 3. Nevertheless, the difference between the velocities gives correctly the larger values of α for the spheroid than for the other sheets of the Fermi surface.

The expression (6) is obtained in the approximation of a spherical Fermi surface and plane-wave electron functions. Figure 2 gives the results of a numerical (computer) calculation of the ee collision frequency for different points on the Fermi surface of W, carried out in the tight-binding

TABLE II.

Surface	Direction of \mathbf{B}	W		Mo	
		$v(k)$, 10^8 cm/sec	k , \AA^{-1}	$v(k)$, 10^8 cm/sec	k , \AA^{-1}
Octahedron	$\langle 100 \rangle$	0,53	0,75	0,50	0,79
	$\langle 111 \rangle$	1,55	0,50	0,72	0,51
	$\langle 110 \rangle$	0,95	0,60	0,76	0,60
Jack	$\langle 111 \rangle$	0,67 *	0,43 *	0,60 *	0,49 *
Spheroid	$\mathbf{B}, \langle 110 \rangle = 24^\circ$	0,52 *	0,25 *	0,45 *	0,31 *

Note. The density $N(\epsilon_F)$ was assumed to be $1.9 \times 10^{31} \text{ erg}^{-1} \cdot \text{cm}^{-3}$ for W and $3.2 \times 10^{34} \text{ erg}^{-1} \cdot \text{cm}^{-3}$ for Mo (Ref. 1).

*These data were obtained from the values averaged over an orbit.

approximation allowing for the real form of the Fermi surface and the electron wave functions.²⁸ We can see that, to within a factor of 1.5, these results are in agreement with our data. It follows from these calculations that the value of α for the spheroid is higher than for other sections of the Fermi surface. Although the authors of Ref. 28 assume that the Born approximation does not overestimate seriously the probability of the ee collisions in W, the existence of the factor of 1.5 does demonstrate that the probability is overestimated.

In the case of compensated metals we can expect a correlation between the coefficient a in the quadratic term of the electrical resistivity $\rho(T)$ and the value of α_{tr} , corresponding to the transport frequency of the ee collisions:

$$\alpha_{tr} = e^2 \langle v_F \rangle S_F a / 6\pi^2 \hbar, \quad (7)$$

where $\langle v_F \rangle$ is the Fermi velocity averaged over the Fermi surface and S_F is the Fermi surface area. The existence of surface-induced deviations from the Matthiessen rule is responsible for the dependence of the coefficient a in the law $\rho = \rho_0 + aT^2 + bT^5$ on the properties of a sample.^{8,9} However, the experiments carried out at ultralow temperatures (0.04–1.5 K) indicate that after freezeout of phonons the purely quadratic law $\rho = \rho_0 + aT^2$ is obeyed and the coefficient a is practically independent of the product $\rho_0 d$. Moreover, an analysis of the influence of the size effect on $\rho(T)$ using a theory allowing for the angular dependence of the specular coefficient p shows that $a = a_{ee} + a(p)$, where $a(p) \approx 0$ for a diffusely scattering surface and $a = f(l/d)$ for $p \neq 0$ (Ref. 11). The value $a_{ee} = 5 \times 10^{-13} \text{ } \Omega \cdot \text{cm} \cdot \text{K}^{-2}$ yields an estimate $\alpha_{tr} = 0.43 \times 10^7 \text{ sec}^{-1} \cdot \text{K}^{-2}$, in agreement with our results. The value of a_{ee} obtained in Ref. 11 is so small that it satisfies the extrapolation of $\rho(T)$ from the "high-temperature" region to $T = 0$ as well as the extrapolation with $a = 0$ used in Ref. 8. Moreover, if a_{ee} includes the contribution of the ee scattering via exchange of virtual phonons, then a_{ee} may decrease on increase in temperature.^{29,30}

In the case of Mo the ee collision frequency is considerably higher than for W: $\alpha_{Mo} = 2.5 \times 10^7 \text{ sec}^{-1} \cdot \text{K}^{-2}$ (Ref. 3), which is due to the higher density of electron states deduced from the linear term in the specific heat (Table II). On the other hand, the ep collision frequency is considerably less because of the difference between the Debye temperatures.¹ A comparison of the Fermi velocities on different sheets of the Fermi surfaces of W and Mo shows that this difference is retained for all the sheets. A simple substitution of the relevant quantities in Eq. (6) shows that the frequency

of the ee collisions in W should be half that in Mo. Subject to the simplifying assumptions made in the derivation of Eq. (6), such an estimate is in good agreement with the experimental data.

The results obtained therefore demonstrates that the temperature dependence of the collision frequency $\bar{\nu}(T)$ is described well by the law $\bar{\nu}(T) = \alpha T^2 + \beta T^3$ with a coefficient α which is isotropic and independent of the magnetic field, frequency, and thickness of a sample. The value of α is in agreement with the theoretical calculations of the ee collision probability and with the transport value α_{tr} deduced from the measurements of $\rho(T)$. This evidence demonstrates that the quadratic term in the dependence $\bar{\nu}(T)$ for W is related specifically to the ee interaction. The RSE method makes it possible to investigate the ee interaction in its pure form not masked by the influence of the size and other effects.

The authors are grateful to V. F. Gantmakher and V. E. Startsev for discussions and valuable comments, to S. V. Plyushcheva for supplying an ingot of ultrapure tungsten, and to L. G. Fedyaeva for her help in the computer calculations.

¹The values of the electrical resistivity ratios of the samples are given incorrectly in Ref. 14.

¹V. V. Boiko, V. F. Gantmakher, and V. A. Gasparov, Zh. Eksp. Teor. Fiz. **65**, 1219 (1973) [Sov. Phys. JETP **38**, 604 (1974)].

²V. F. Gantmakher and I. B. Levinson, Zh. Eksp. Teor. Fiz. **74**, 261 (1978) [Sov. Phys. JETP **47**, 133 (1978)].

³M. A. Arutyunyan and V. A. Gasparov, Zh. Eksp. Teor. Fiz. **76**, 369 (1979) [Sov. Phys. JETP **49**, 188 (1979)].

⁴V. A. Gasparov, I. F. Voloshin, and L. M. Fisher, Solid State Commun. **29**, 43 (1979).

⁵V. A. Gasparov and S. A. Kozlov, Pis'ma Zh. Eksp. Teor. Fiz. **34**, 122 (1981) [JETP Lett. **34**, 115 (1981)].

⁶J. A. Rayne and K. K. Leibowitz, J. Phys. (Paris) **39**, Colloq. 6, C6-1006 (1978).

⁷B. P. Nilaratna and A. Myers, J. Phys. (Paris) **39**, Colloq. 6, C6-1064 (1978).

⁸V. I. Cherepanov, V. E. Startsev, and N. V. Vol'kenshtein, Fiz. Nizk. Temp. **6**, 890 (1980) [Sov. J. Low. Temp. Phys. **6**, 432 (1980)].

⁹V. E. Startsev, V. P. Dyakina, V. I. Cherepanov, N. V. Vol'kenshtein, R. Sh. Nasyrov, and V. G. Manakov, Zh. Eksp. Teor. Fiz. **79**, 1335 (1980) [Sov. Phys. JETP **52**, 675 (1980)].

¹⁰C. Uher, M. Khoshnevisan, W. P. Pratt Jr., and J. Bass, J. Low Temp. Phys. **36**, 539 (1979).

¹¹J. van der Maas, R. Huguenin, and V. A. Gasparov, J. Phys. F **15**, L271 (1985).

¹²T. Moriya, J. Magn. Magn. Mater. **14**, 1 (1979).

¹³V. A. Gasparov, I. F. Voloshin, and L. M. Fisher, Abstracts of Papers presented at Twenty-Second All-Union Conf. on Low Temperature Physics, Kishinev, 1982 [in Russian], Part 2, p. 123.

¹⁴I. F. Voloshin, V. G. Skobov, L. M. Fisher, and A. S. Chernov, Zh. Eksp. Teor. Fiz. **82**, 293 (1982) [Sov. Phys. JETP **55**, 175 (1982)].

- ¹⁵V. V. Boiko and V. A. Gasparov, Zh. Eksp. Teor. Fiz. **61**, 1976 (1971) [Sov. Phys. JETP **34**, 1054 (1972)].
- ¹⁶V. A. Gasparov, P. A. Probst, R. Stubi, and R. Huguenin, Proc. Intern. Conf. on Localization, Interactions, and Transport Phenomena in Impure Metals, Brunswick, West Germany, 1984 (ed. by B. Kramer, G. Bergmann, and Y. van Bruynseraede), Springer Verlag, Berlin (1985), p. 260 [Springer Series in Solid-State Sciences, Vol. 61].
- ¹⁷J. B. Ketterson, D. D. Koelling, J. C. Shaw, and L. R. Windmiller, Phys. Rev. B **11**, 1447 (1975).
- ¹⁸V. V. Nemoshkalenko, A. V. Zhalko-Titarenko, and V. N. Antonov, Fiz. Nizk. Temp. **9**, 1249 (1983) [Sov. J. Low Temp. Phys. **9**, 642 (1983)].
- ¹⁹V. F. Gantmakher, Rep. Prog. Phys. **37**, 317 (1974).
- ²⁰D. K. Wagner and R. Bowers, Adv. Phys. **27**, 651 (1978).
- ²¹P. J. Feenan, A. Myers, and D. Sang, Solid State Commun. **16**, 35 (1975); D. Sang, A. Myers, and P. J. Feenan, *ibid.* **18**, 597 (1976).
- ²²R. Herrmann and V. S. Edel'man, Zh. Eksp. Teor. Fiz. **53**, 1563 (1967) [Sov. Phys. JETP **26**, 901 (1968)].
- ²³R. Herrmann, Phys. Status Solidi **25**, 661 (1968).
- ²⁴V. A. Gasparov and M. H. Harutunian, Phys. Status Solidi B **93**, 403 (1979).
- ²⁵D. E. Soule and J. C. Abele, Phys. Rev. Lett. **23**, 1295 (1969).
- ²⁶V. A. Gasparov, J. Lebeck, and K. Saermark, J. Low Temp. Phys. **50**, 379 (1983).
- ²⁷K. Dobson and A. Myers, Solid State Commun. **35**, 27 (1980).
- ²⁸C. Potter and G. J. Morgan, J. Phys. F **9**, 493 (1979).
- ²⁹A. H. MacDonald, Phys. Rev. Lett. **44**, 489 (1980).
- ³⁰A. H. MacDonald, R. Taylor, and D. J. W. Geldart, Phys. Rev. B **23**, 2718 (1981).

Translated by A. Tybulewicz